RSC Advances

ROYAL SOCIETY OF CHEMISTRY

www.rsc.org/advances

ARTICLE TYPE www. rsc.org/xxxxxx | XXXXXXXX

Magnetron sputtered Cu doped SnS thin films for improved photoelectrochemical and heterojunction solar cells†

Malkeshkumar Patel,[a] and **Abhijit Ray**[*a]

Received Xth XXXXXXXXXX 20XX, Accepted Xth XXXXXXXXX 20XX
First published on the web Xth XXXXXXXXXX 200X
DOI: 10.1039/b000000x

Tin (II) sulfide (SnS) is a promising low cost photovoltaic material for its favorable direct optical band gap (~1.3 eV) and high absorption coefficient (> 10^4 cm^{-1}). However, the SnS solar cells are reported to have low efficiency due to band misalignment that can be reduced by a proper optimization of acceptor concentration in p-SnS. This work describes the effect of extrinsic Cu doping in sprayed SnS thin films on SnO_2:F glass for a possible enhancement in the photocurrent in photoelectrochemical and the open circuit voltage in heterojunction solar cells. The structural, morphological, optical and photoelectrochemical properties of Cu:SnS films are studied in details. A process temperature of 325°C was found optimum for the Cu doping at the Sn vacancies in the host lattice. An improvement in the photo-current density from 1.1 mA/cm^2 to 1.8 mA/cm^2 was observed in the photoelectrochemical cell by this doping process. It shows a further enhancement in photocurrent up to 3.2 mA/cm^2 when the residual surface Cu was removed by HCl etching. The developed Cu:SnS heterojunction solar cell showed a record open circuit voltage of 462 mV with In_2S_3 as a buffer layer.

1 Introduction

Tin (II) sulfide (SnS) is a low cost alternative to photovoltaic absorber[1] as well as a photoelectrode for water splitting[2]. It is a p-type semiconductor with direct optical band gap ~1.3eV and high absorption coefficient ~10^4 cm^{-1}.[1,3] As n-type heterojunction partner in solar cells, various buffer materials are possible, such as CdS, In_2S_3, ZnS etc. However, its performance is limited by the band offset between the heterojunction candidates.[4] A negative (type-II) conduction band offset (CBO), is common in most of the cases. Doping of SnS extrinsically can modify the band positions and gap of SnS, leading to either a reduction in negative CBO or creation of a small positive CBO (type-I configuration).[5] Doping at the Sn-vacancy site can change acceptor concentration as well in SnS. The band gap narrowing of p-SnS in type-II heterojunction creates severe effect on the valence band offset (VBO) than that in type-I. When the acceptor concentration approaches 10^{18} cm^{-3}, it becomes a 'broken-gap' (type-III) arrangement.[6] An optimization of doping therefore is required to manipulate CBO as well as VBO in the SnS heterojunction solar cells.

An intrinsically doped SnS shows p-type conductivity. However, it can be modified by changing the Sn/S ratio. The Abinitio studies have shown that the Sn vacancies act as shallow acceptor giving rise to a p-type conductivity, whereas the Sn on S antisites act as donor defects. Hence, the S rich growth condition should be avoided.[7] The p-type conductivity is required for the ideal absorber layer application in the thin film solar cells. While growing the SnS material, the scope of controlling the hole concentration by changing the Sn/S ratio is restricted.[7] The desired hole concentration of SnS material can be achieved by ex-situ doping by pure metals such as, Cu,[5,8] Ag,[9–11] In,[12,13] Al[14] and Pb[15]. SnS can be n-type by doping with Bi[16] and Sb[17,18]. By diffusion of Bi and Sb in the p-type SnS, homojunction solar cell can be feasible. Most studies evidence the resistive nature of SnS layers. The extrinsic doping can adjust this acceptor concentration (N_A) to give a right band gap in the type-II configuration. It has been reported that an optimum acceptor concentration in SnS between 1.5×10^{15} to 8.6×10^{19} cm^{-3} is possible by Cu-diffusion in thermally evaporated SnS film on glass substrate.[5,8]

A potential of 1.23 V is needed for water splitting under standard conditions from a thermodynamic standpoint, therefore a semiconductor with a minimum band-gap, E_g = 1.23 eV (an absorption wavelength cut-off of 1008 nm) could be effective in such application. Based on the standard AM1.5G solar spectrum (1000 Wm^{-2}), a semiconductor with such a band-gap would operate at a maximum overall solar-to-hydrogen conversion efficiency, η_{STH} = 47.4% assuming there exists 100% quantum conversion efficiency and no other losses in the system.[19,20] Therefore, SnS can offer the possibilities of deploying in water splitting application as well. Recently,

† Electronic Supplementary Information (ESI) available: [details of any supplementary information available should be included here]. See DOI: 10.1039/b000000x/

[a] *School of Solar Energy, Pandit Deendayal Petroleum University, Raisan, Gandhinagar 382 007, Gujarat, INDIA. Fax: +91 7923275030; Tel: +91 7923275304; E-mail: abhijit.ray1974@gmail.com*

Sun *et al.* have demonstrated that the all surface atomic SnS sheet based photoanode has a photon to current conversion efficiency of 67.1% at 490 nm with overall photocurrent density of 5.27 mA/cm^2. However, the photocurrent was less than 0.2 mA/cm^2 for bulk SnS (thickness more than 200 nm).[2] The earth abundant SnS semiconductor is composed of weakly interacting layers held together by van der Walls interactions, where in each monolayer, Sn and S atoms are tighly bound by chemical bonds with 100% exposed surface atoms. Moreover, no surplus charge is present on the chemically stable surface of SnS monolayer that are devoid of dangling bonds or surface density of states.[2,5,21]Therefore, achieving a higher photocurrent in bulk SnS (thickness more than 200nm) remains a challenge and may be addressed by a proper doping scheme.

In the present study, thin film of SnS developed by a compressed air assisted chemical spray pyrolysis (CSP) was doped with Cu by pulsed DC-magnetron sputtering. The Cu:SnS thin films were characterized for their crystal structure, morphology, elemental composition, electrical and optical properties. Copper was doped ex-situ in to SnS by varying the substrate temperature. Our results show an improvement in the photocurrent density in the photoelectrochemical cell and an exceptional rise in open circuit voltage in the doped SnS thin films solar cell. This doping scheme will be useful in developing solution processed SnS solar cells with higher efficiency over the existing efficiency of 1-2%.[1,22,23]

2 Results and discussion

2.1 Structural and phase analysis

The XRD pattern of as spayed and doped at different temperature from 275°C to 350°C for fixed sputtering parameters is shown in Fig. 1. The observed XRD spectra used to determine the phases, lattice parameters, space group and dimension of unit cell. The dominant peak broadening of characteristic phase is used to estimate the strain and crystallite size. The SnS material was considered to have orthorhombic crystal symmetry with different space group of *Pbnm* (62) and *Cmcm* (63) according to COD-AMSCD data. The unit cell of SnS material having a space group of *Pbnm* (62) is shown as an inset of Fig. 1. The XRD data were processed as described elsewhere.[24] The background-corrected XRD patterns of all the sprayed films after performing the phase analysis reveal peaks corresponding to the (110), (120), (021), (101), (111), (040), (131) and (152) planes of reflection, which are the characteristics of the SnS phase having the *Pbnm* orthorhombic symmetry. The ideal planes of reflection of COD-AMCSD 900-8785 is shown in Fig. 1. The as sprayed SnS film appears as mix phase of *Pbnm*(62) and *Cmcm*(63) (COD-AMCSD-900-8295) symmetries. The (021) plane of reflection is corresponding to the *Cmcm*(63) space group. The XRD profiles of the SnS

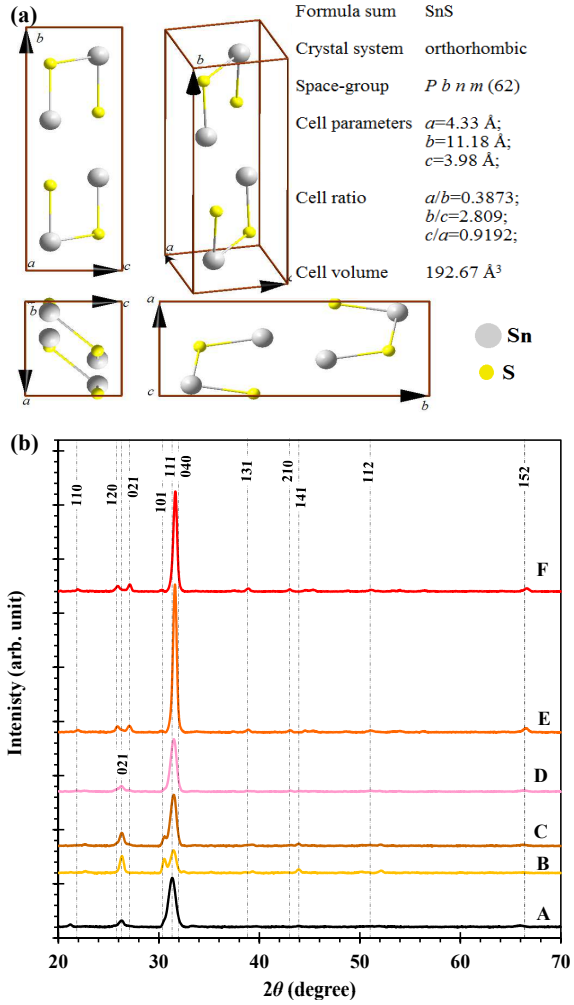

Fig. 1 Effect of Cu doping on the structural properties of sprayed SnS film. (a) Isometric view of orthorhombic unit cell of SnS material (COD: 900-8785) and (b) effect of Cu diffusion due to various annealing temperature on the XRD patterns.

Table 1 Summary of structural properties (2θ, $FWHM$, d-spacing, lattice parameters, crystallite size and micro strain) of as deposited and Cu doped SnS thin films

Sample code	Substrate temperature (°C)	2θ (°)	$FWHM$ (°)	d-spacing (Å)	Lattice constants (Å)			grain size t (nm)	micro strain Δ
					a	b	c		
900-8765	-	31.538	-	2.834	4.33	11.18	3.98	-	-
A	as-spayed	31.387	0.931	2.847	4.35	11.23	4	9.84	3.910
B	35	31.517	0.81	2.836	4.33	11.19	3.98	11.32	3.401
C	275	31.53	0.71	2.835	4.33	11.18	3.98	12.92	2.981
D	300	31.527	0.717	2.835	4.33	11.18	3.98	12.79	3.010
E	325	31.661	0.401	2.823	4.31	11.14	3.97	22.88	1.683
F	350	31.696	0.405	2.821	4.31	11.13	3.96	22.65	1.700

crystal structure with space group of *Pbnm* (62) and *Cmcm* (63) were generated by Pseudo-Voigt function from the crystallographic information files (COD: 600-8285 and 600-8295) and they shown in Fig. S3† and S4†. The detail of samples A to F is provided in the Table 1, where the substrate temperature of Cu diffusion is a parameter. It is interesting to note that the mix phase appearance of SnS film was removed for the samples E and F. In all the cases, (111) planes remains a preferentially oriented one. It was revealed from the peak analysis that the SnS phase is not affected by the doping process. It is important to check whether Cu was doped by substitution or interstitial site. The Cu peak ($2\theta = 43.3°$; COD-AMCSD-710-1264) is anticipated, if Cu goes to the interstitial sites of SnS planes, however no peak corresponds to Cu was found. Which may indicates a substitutional doping of Cu at Sn vacancies of SnS. Other impurity phases such as, Cu_2SnS_3, Sn_2S_3 and SnS_2 were not detected in the deposited films during the Cu diffusion by sputtering.

The finite size of the crystallite causes a broadening of the diffraction lines which can be related to its size by the Debye-Scherrer formula,[25] where the micro strain of the films was obtained using this relation.[26] In thin films, the residual strain may occur at the scale of microstructure and crystal structure, which are, by necessity, balanced by stresses in the other locations or crystal planes within the material for an equilibrium configuration.[27] XRD data can determine the residual strain only at the level of crystal structure. The intergranual micro stress can be determined by optical interferometric method. However, both types of strain measurement on same sample are rarely found.[28] The estimated d-spacing, crystalline size (t) and residual strain (Δ) for all the films are listed in Table 1. From Fig. 1 and Table 1, the shift of the (111) peak position to the higher θ value from 31.387° to 31.696° indicates the existence of crystal lattice compression after Cu-doping. This confirms the compressive nature of micro-strain. As a result, the lattice volume was decreased from 192.67 Å^3 to 189.87 Å^3 as Cu gets diffused in SnS lattice. Therefore, the unit cell volume reduction in the temperature range 275°C - 350°C during the sputtering was probably due to the substitution of smaller Cu^{2+} for larger Sn^{2+} site. From the XRD spectra, the substrate temperature of 325°C was found to be optimum for the Cu doping in SnS.

2.2 Microstructure and elemental analysis

Table 2 Summary of the elemental analysis of as deposited and Cu doped SnS thin films

Sample code	Atomic percentage (%)			Sn/S	(Cu+Sn)/S
	Sn	S	Cu		
A	51.57	48.43	-	1.065	-
B	31.38	30.57	38.05	1.026	2.271
C	16.27	38.3	45.43	0.425	1.611
D	25.42	42.16	32.42	0.603	1.372
E	32.3	48.41	19.41	0.667	1.068
F	34.75	52.24	13.01	0.665	0.914

Fig. 2 shows the topographical FESEM images of the as deposited and Cu doped SnS films at various diffusion temperature. The obtained microstructure is in agreement with the reported SnS thin films synthesized using the vacuum techniques such as, atomic layer deposition,[21] thermal evaporation[22] and sputtering.[29] Fig. 2(a) showed the morphology of as sprayed SnS film as represented by the vertically oriented petal like polycrystalline grains propagating almost vertically to the surface. The average length of the petal kind microstructure was measured to be 500 nm in the horizontal direction. The sputtered Cu thin layer (~100 nm) on the SnS can be observed from the topography image in Fig. 2(b). It was identical to that of Cu thin layer on the glass substrate (please refer the Fig. S7†, where FESEM topography of sputtered Cu layer on the glass substrate with different magnification shown). The Cu diffusion while sputtering is observed to be diffused into SnS layer and its' transition from surface to bulk can be observed from in Fig. 2(c)-(f). The Cu doping at 325°C of substrate temperature while sputtering found to be optimum for the denser SnS films and visible Cu fraction could not be observed from the topography. The thickness of each sam-

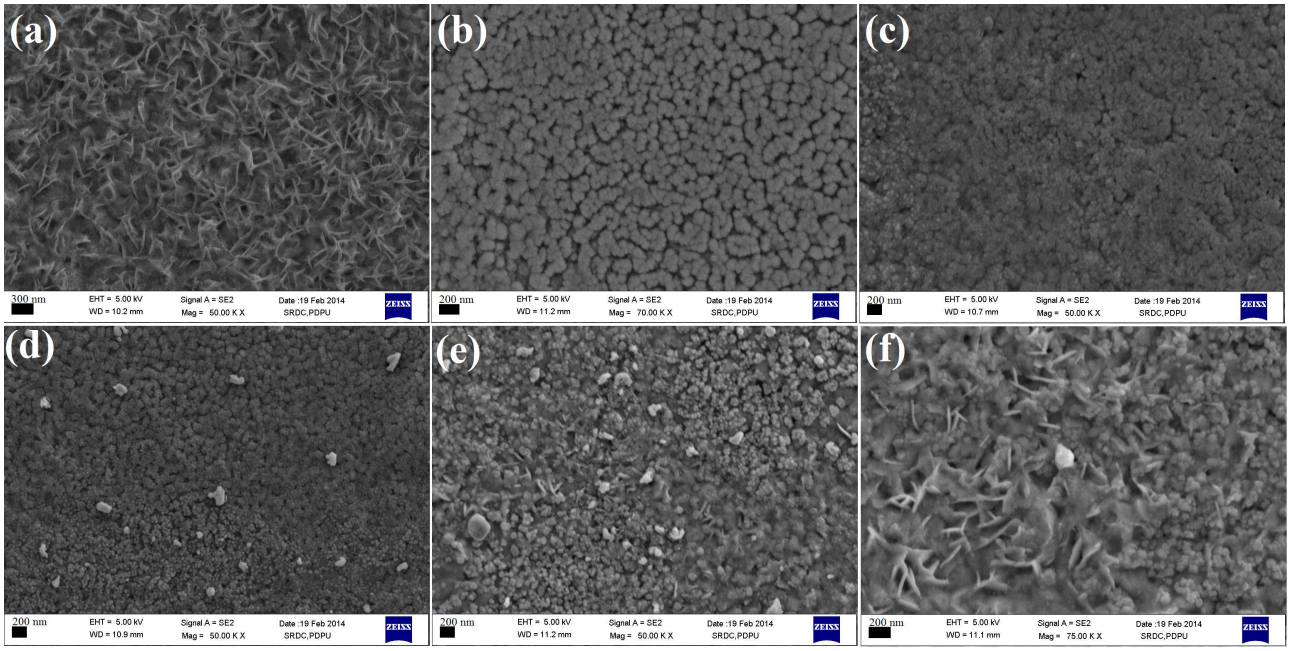

Fig. 2 Surface topographical FESEM images of 500 nm thick (a) undoped and magnetron sputtered Cu on spayed SnS at different temperatures, (b) 35°C, (c) 275°C, (d) 300°C, (e) 325°C and (f) 350°C on glass substrate.

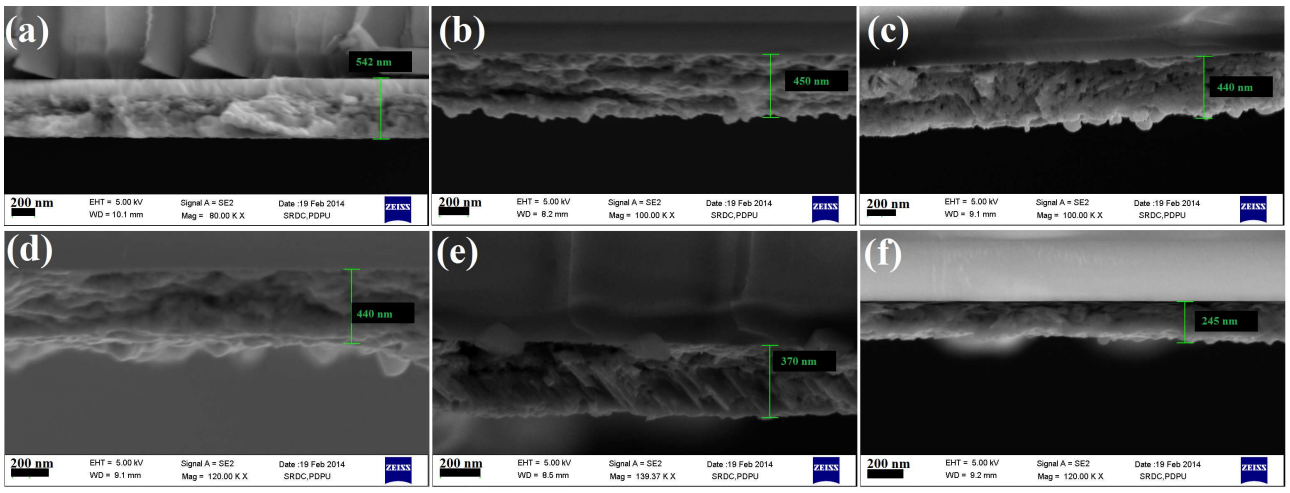

Fig. 3 Cross sectional FESEM images of samples A-F (a) undoped and magnetron sputtered Cu on spayed SnS at different temperatures, (b) 35°C, (c) 275°C, (d) 300°C, (e) 325°C and (f) 350°C on glass substrate.

ple was estimated by cross sectional FESEM image analysis as shown in Fig. 3. Non uniformity is a common issue with thin films processed by most of the non-vacuum techniques. The ex-situ doping process has a special advantage with the solution processed thin films, which assist in an easy diffusion into the structure. Our FESEM images revealed that the morphology of SnS films was modified due to Cu diffusion in to the SnS material. However, Cu doped films remained pinhole free (Please refer the Fig. 2). The cross section FESEM images (Fig. 3) had revealed the similar observation for Cu doped SnS on glass substrates. The summary of elemental (EDS) analysis is provided in Table 2, where the atomic percentage of Sn, S and Cu are given. The Sn/S ratio of the as prepared and Cu deposited at room temperature is in agreement and was near to ~1. The as-deposited SnS material was Sn rich intrinsically. The EDS analysis revealed that the SnS material doped by sputtered Cu at 325°C of temperature and Cu took the Sn site in the lattice. The ratio of (Sn+Cu)/S are in agreement with Sn/S of sample A. The EDS in the cross-section of Cu:SnS was performed to investigate the diffusion profile. The result is shown in Fig. 4. It shows a consistent distribution of Cu in the SnS layer because of a diffusion process taking place at an optimum temperature of 325°C. Here it is shown for the Cu:SnS/FTO processed at 325°C of diffusion temperature for 30 minutes.

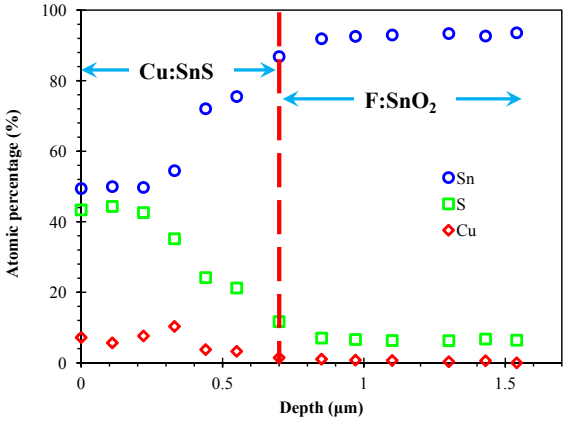

Fig. 4 The depth profile of Cu:SnS on the FTO coated glass substrate, shows the concentration distribution of elemental percentage of Sn, S and Cu.

2.3 Optical properties

The absorption co-efficient (α), Tauc plot and derivative of $ln(h\nu\alpha)$ with respect to $h\nu$ for samples A-F are shown in Fig. 5(a), (b) and (c), respectively. The thickness of SnS layer, absorption co-efficient, optical band gap (E_g) and absorption length ($L = 1/\alpha$) of each samples are summarized in Table 3.

Table 3 Summary of optical property of un-doped and Cu doped SnS thin films on glass substrate. The thickness of each samples were determined by FESEM analysis. Please refer Fig. 3, where the thickness of Cu doped SnS later on glass substrate are shown

Sample code	Thickness (nm)	E_g (eV)	α ($\times 10^4$ cm^{-1})	$L = 1/\alpha$ (nm)
A	550	1.44	1.4	715
B	520	1.84	7.8	128
C	400	1.42	2.9	345
D	370	1.5	3.4	295
E	350	1.66	7.2	140
F	330	1.48	4.1	244

The transmittance and absorption spectrum of SnS films are provided in the Fig. S6(a)[†] and (b)[†] of ESI, respectively. The method of estimation of α and E_g is provided elsewhere.[24,30] The band gap was estimated by Tauc as well as by derivative, $d(ln(h\nu\alpha))/d(h\nu)$ methods. The later provided a more accurate value of E_g and therefore considered in our study. The results are consistent with the published data. From the XRD and FESEM, it was revealed that Cu was doped in SnS by the diffusion process in the temperature range of 325°C-350°C. Therefore, we analyzed the optical properties of the samples processed in this range of temperature only. The estimated absorption coefficient (α) in the Cu doped film was found to enhance by a factor of 5.4 in the annealed film from that of 1.4 $\times 10^4$ cm^{-1} in case of the as-prepared film. It reveals that only 140 nm thick Cu:SnS can absorb most of the incident photons having their energy greater than 1.6 eV. The estimated α for sample E was maximum. The E_g of as prepared SnS film was 1.44 eV. By the Cu doping in SnS material, the band gap was increased and reached up to 1.66 eV. Therefore, a blue shift in the optical band gap is observed as an effect of Cu doping, confirming that there are no deep defect state that has been created due to Cu. The similar observation was made by Gremenok *et al.* for Pb doped SnS where E_g was increased from 1.22 eV to 1.32 eV by Pb doping.[15] Moreover, similar shift in E_g was observed from 1.34 eV to 1.43 eV by Ag doping in SnS material.[11] The abinitio study, in the contrary suggests that the indirect E_g should decrease from 0.982 eV to 0.864 eV by replacing a Sn atom by Cu.[5] Such a band gap reduction was reported only for Al as a dopant in SnS where E_g was reduced from 1.5 eV to 1.29 eV.[14]

2.4 Photo response (Photoelectrochemical cell and heterojunction solar cell)

Photoelectrochemical (PEC) cell response of the undoped and Cu doped SnS films on the FTO glass substrate with $K_4Fe(CN)_6$ +$K_3Fe(CN)_6$ electrolyte was recorded using linear sweep photo voltammogram technique. The topography

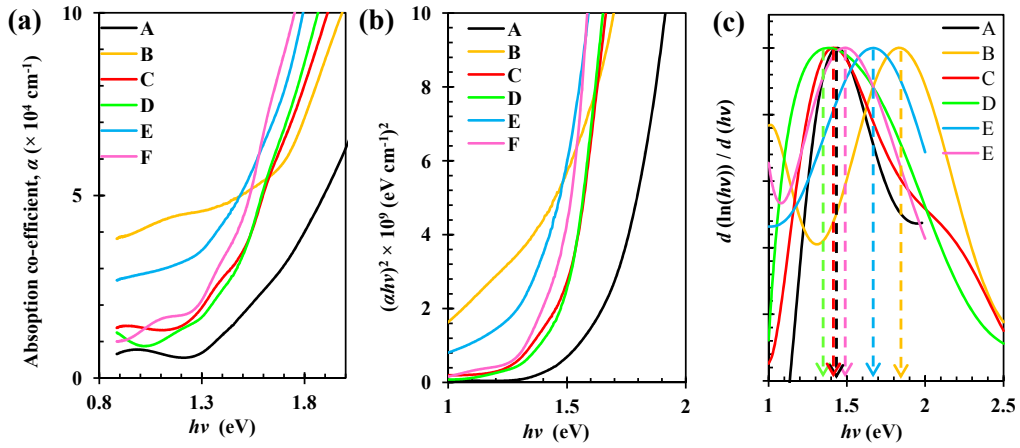

Fig. 5 Optical properties of undoped and Cu doped SnS thin films on glass substrate (a) absorption coefficient, (b) Tauc plot and (c) first derivative plot of normalized value of $d(\ln(h\nu\alpha)) / d(h\nu)$.

and cross section morphology of SnS/FTO photocathode is shown in Fig. 6. The thickness of fabricated Cu doped SnS working electrode was 600 nm (Fig. 6(c)). The steady state light and dark *J-V* envelops of constructed PEC cell of Cu doped SnS electrode is presented in Fig. 7. The PEC cell was illuminated by pulsed high power white LED light from the front side, where forward bias voltage was applied. The photo response of PEC cell consists of working electrode of as deposited SnS, Cu:SnS and after HCl treatment are shown in Fig. 8. In this case the photo generated carriers are collected due to the electric field present at the semiconductor-electrolyte interface. The flat band potential (V_{FB}), photo current density at zero bias and maximum photo current density at a given bias voltage is summarized in the Table 4. A flat band potential of 0.38-0.48 V was identified from the PEC response. A significant improvement in PEC response was found for Cu doped SnS film as compared to the pristine film. According to the observed cathodic photocurrent of PEC, all the films were photoactive and p-type in nature. The dark and light envelop of *J-V* (vs. Ag/AgCl) of Cu doped SnS electrode is presented in Fig. 7, where the photogenerated current density of 1 mA/cm^2 at zero bias and 1.8 mA/cm^2 at a bias of -0.15 V vs. Ag/AgCl is highlighted. The achieved photogenerated current density was 0.65 mA/cm^2 higher than that in reported SnS electrode grown by electrodeposition. The improvement in dark current and photogenerated current density can be attributed to the enhanced build in potential because of the improved carrier concentration of the SnS material on the FTO substrate. The summarized electrochemical cell parameters are provided in the Table 4. The atomic layer thin intrinsic SnS (less than 200 nm) electrode employed for water splitting application offered the maximum current density of 5.27 mA/cm^2 for the applied potential of 0.6 V vs. Ag/AgCl reference electrode.[2] This large photocurrent is mainly attributed to n-type conductivity of atomic layer thin SnS material, however, the bulk thin film of SnS shows a photocurrent density of 0.05 mA/cm^2. The dark current for the Cu doped SnS films shows large magnitude at the applied bias more than the flat band potential. From the EDS analysis, it was revealed that the trace of elementary Cu was found on the surface of SnS material, which was yet to be diffused. This residual Cu could be removed by HCl treatment. It was evident from the distinct shaped grains of Cu-doped SnS in Fig. 6(b) as compared to that of as prepared SnS in Fig. 6(a). The dark current was found to be much reduced after the HCl treatment. The removal of Cu from the surface provided a better semiconductor electrolyte interface. As an effect, a larger photocurrent density of 3.2 mA/cm^2 was obtained for the applied potential of -0.42 V vs. Ag/AgCl reference electrode. The obtained larger photocurrent is therefore attributed to the improved N_A. EDS analysis revealed that the Cu was present into SnS even after the HCl treatment, therefore the HCl treatment did not affect the Cu at the doping site in the SnS material.

Table 4 The estimated parameters from the PEC response of undoped and Cu doped SnS thin films over the FTO coated glass substrates are summarized here. The photo-generated current density $J_{photo} = J_{light} - J_{dark}$. Current density is in mA/cm^2

Sample	V_{FB}	J_{dark}	J_{photo} at V=0	J_{photo} (max)
As deposited	0.49	0.2	1	1.1
Cu:SnS	0.5	0.1	1.2	1.7
Cu:SnS(Etched)	0.38	0.01	1.5	3.2

The *J-V* characteristics of grown SnS and Cu:SnS solar cells having the In_2S_3 as buffer layer is shown in Fig. 9. The cross section of the grown SnS solar cell is shown in Fig. 6(d).

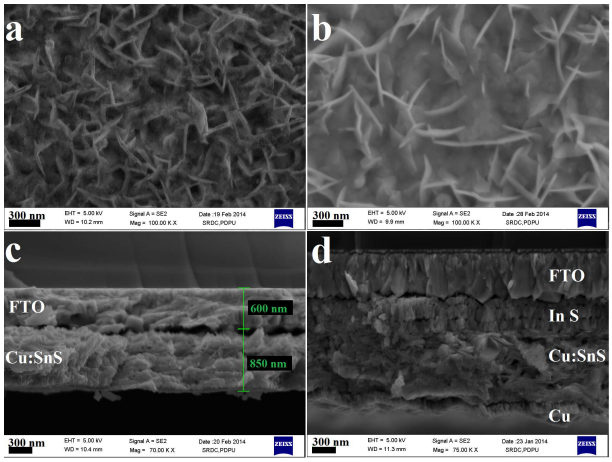

Fig. 6 The FE-SEM topographic image of (a) undoped SnS and (b) Cu-doped SnS. The cross sectional FE-SEM images of (c)Cu-doped SnS and (d) heterojunction solar cell on FTO substrate.

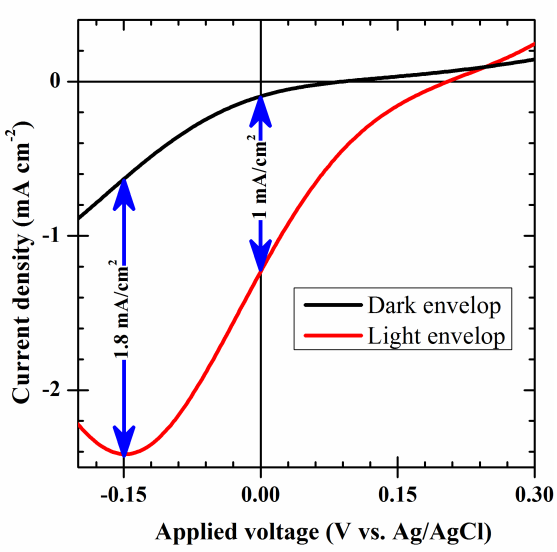

Fig. 7 Dark and light envelop of constructed photoelectrochemical cell of Cu doped SnS electrode on FTO substrate.

All the layers of are distinguished. The estimated thickness of SnS layer is 700 nm. The V_{OC} of 210 mV is enhanced 462 mV over as grown SnS solar cell. The achieved V_{OC} of 462 mV is the highest in its' class of solar cell. This improvement is because of the enhanced N_A of SnS layer. The enhanced V_{OC} may be attributed to the local degenerate nature of SnS close to the surface causing a back surface filed by the Cu doping. However, the EDS analysis revealed the equal diffusion of Cu in to SnS layer as 325°C of deposition temperature. The diffusion temperature of Cu had an influence on the performance of solar cell. It was found that a diffusion temperature more than 350°C could reduce the shunt resistance and hence solar cell performance. The efficiency of the developed Cu doped SnS solar cell is limited by the poor fill factor. Given a further direction to improve the fill factor, would improve efficiency of this low cost solar cell to a substantial level.

3 Experimental

3.1 Thin films deposition by spray pyrolysis

Thin film of tin (II) sulfide was prepared by the spray pyrolysis technique using aqueous solution of as received $SnCl_2{\cdot}2H_2O$ (SC) (> 99%) and Thiourea (TU) (> 99%). The optimized molar concentration ratio of 1:1.25 of SC/TU was maintained. We have added 0.55-0.65 ml of HCl (35-38% LR, S D Fine Chem Ltd.) to enhance the solubility of 0.05M $SnCl_2{\cdot}2H_2O$. The F:SnO_2 (FTO) coated glass substrates (of sheet resistance 15 Ω/□ , area 0.5 × 1.5 cm^2 and thickness 2.2 mm) were thoroughly cleaned as described elsewhere.[24] All chemicals and substrates were procured from Sigma Aldrich and used without any further purification. Prepared aqueous chemical solution was transported to the spray nozzle from a syringe pusher and sprayed on the glass substrate in ambient atmosphere. The process parameters and details of CSP are described elsewhere[24] provided the temperature of the glass substrates was maintained at 375±5°C during the spray. After the spray, the substrate was naturally cooled down to 50°C and then removed from the spray station. The films appeared to be dark red in day light transmission.

3.2 Cu doping by pulsed DC magnetron sputtering

The sprayed SnS thin films on FTO and glass substrates were loaded inside a pulsed DC magnetron sputtering deposition system procured from Milman Inc. for Cu deposition and ex-situ diffusion. The Cu target (purity > 99.999%) was sputtered at different procured from Milman Inc. The target was DC sputtered under Argon plasma at 10 W of power with 50% of duty with pulsed frequency of 10 kHz. The ultimate pressure of 3 × 10^{-5} mbar was achieved by running turbo molecular pump backed with rotary pump. The sputtering pressure of 6.5 × 10^{-3} mbar was maintained by flowing Ar (purity > 99.999%) gas at the flow rate of 20 SCCM. 100 nm of Cu at the deposition rate of 60Å m^{-1} was deposited at room temperature of (35°C) on the 500 nm thick SnS layer and then to allow Cu diffusion in the SnS layer, substrate temperature was varied from 275°C to 350°C to find an optimum temperature of diffusion. Thickness of Cu was monitored through thickness/rate monitor of Inficon (model, SQM-160).

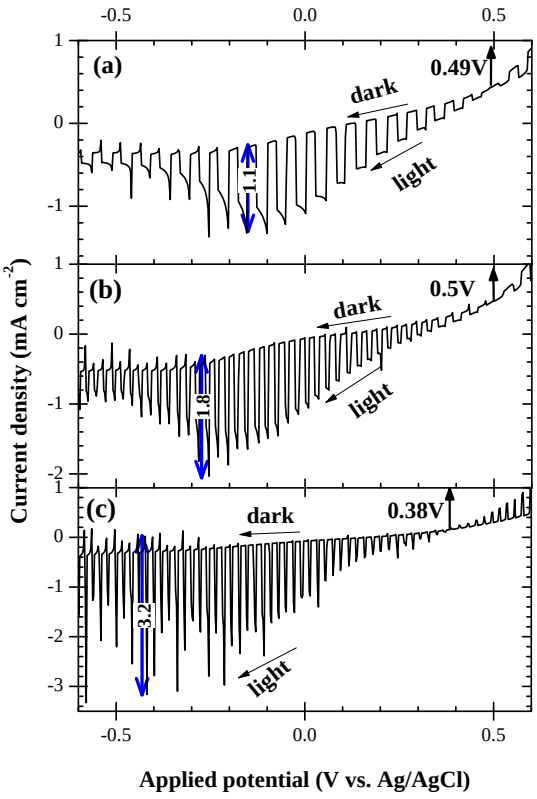

Fig. 8 The linear sweep photo-voltammogram under pulsed illumination of undoped and Cu doped SnS- $K_4Fe(CN)_6$ + $K_3Fe(CN)_6$ electrolyte interface in the forward and reverse bias regime. (a) as deposited SnS film, (b) Cu doped SnS at 325°C of diffusion temperature and (c) after HCl treatment. The scan direction of potential was from positive to negative.

3.3 Material characterization

The structural characterization of the SnS thin film was carried out by X-ray diffractometer from PANalytical (model, X'Pert Powder) with Cu-K_α radiation, $\lambda_{K\alpha}$ = 1.540598 Å, step size = 0.05, and time/step size = 0.5 s/step in 'Gonio mode'. The thickness and average surface roughness of SnS films were characterized by a surface profiler of Vecco (model, Dektak 150). The planar and cross sectional morphology were analyzed by field emission scanning electron microscope (FE-SEM) of Zeiss (model, Ultra 55) with 5 kV of field voltage using SE2 detector. The elemental composition of the as-prepared film was determined by energy dispersive spectroscopy (EDS) attached to the SEM with field voltage of 20 kV. Optical characterization was carried out by a UV-vis spectrophotometer of Shimadzu (model, UV-2600) by recording the transmission spectra of the thin films in the range 320-1400 nm. The extrinsic nature of type of conductivity of the films was determined using the hot point probe method.

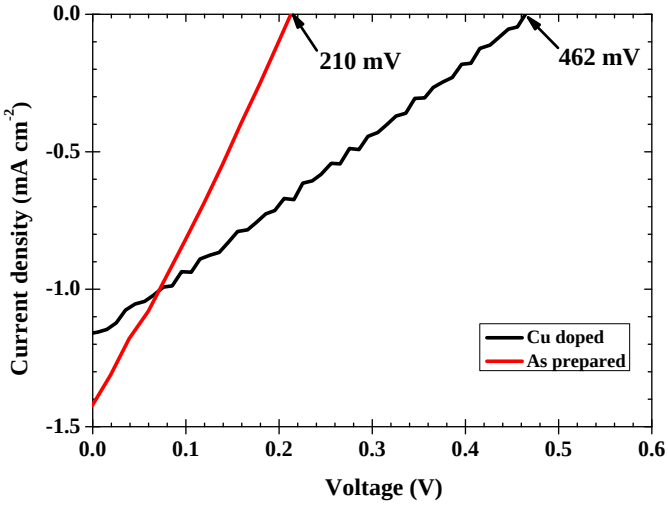

Fig. 9 The *J-V* characteristics of undoped and doped SnS solar cell under AM1.5G.

3.4 Photoelectrochemical and heterojunction solar cell

The SnS-based photoelectrochemical (PEC) cells were fabricated with spray deposited SnS over FTO coated glass substrate in same technique as described above, where 50 ml of 0.1 M ($K_4Fe(CN)_6$) + 0.01M $K_3Fe(CN)_6$ aqueous solution has been used as electrolyte. A PEC solar cell having configuration Pt (2 cm^2) | 0.1 M ($K_4Fe(CN)_6$) + 0.01 M $K_3Fe(CN)_6$ | SnS (0.25 cm^2) — FTO was constructed. The current voltage profile under chopped light illumination condition was recorded by Autolab potentiostat/galvanostat using Ag/AgCl as reference electrode. The film surface inside the PEC cell was illuminated by white high power LED from Wenrun (product, WR-EC150150UW-1000C-9P40) excited (600 W m^{-2}) at 12 V DC with manual chopper of frequency 2 Hz. The active area of the SnS electrode was 5 mm × 5 mm kept fixed for all experiments. The heterojunction of undoped and doped SnS solar cell was fabricated with In_2S_3 buffer layer as described elsewhere (The device fabrication scheme is illustrated in the Fig. S5†, this process were explored for the development of superstrate configured SnS solar cell).[31,32] Please refer Fig. S1† and S2†, where structural and optical characterization of In_2S_3 buffer layer has been shown, respectively. The *J-V* characteristics were recorded by a source measure unit from Agilent (model, U2722A), combined with a AAA class solar simulator from Photo Emmision Tech Inc. (model, SS80) under AM1.5G illumination condition. The light intensity was calibrated by the certified stan-

dard silicon reference cell.

4 Conclusions

In conclusions, we have deposited high quality SnS films on glass and FTO coated glass substrates by most affordable chemical spray pyrolysis method using ambient air assisted transport of aqueous solution of Sn^{2+} and S^{2-}. The SnS are doped by pulsed DC magnetron sputtering of elemental Cu as different temperature. The 325°C of substrate temperature is optimum for Cu diffusion in the SnS layer, where Cu going to substitute sites of Sn vacancies. Our result demonstrates the good control over the structural, morphological, optical and optoelectronic properties of Cu doped SnS films. The significant improvement in the *FWHM* of 0.4° is obtained for Cu doped SnS thin film at 325°C of process temperature. The observed morphological properties of SnS films are identical of films grown by CVD, thermal evaporation and sputtering processes. The photo generated current density of 1.8 mA/cm^2 is achieved for constructed electrochemical cell having an active area of 0.25 cm^2, which shows a further improvement up to 3.2 mA/cm^2 after HCl etching. The enhanced acceptor carrier concentration due to Cu doping has caused a high V_{OC} of 462 mV in Cu:SnS/In_2S_3 heterojunction device which is more than double that of an un-doped case.

Acknowledgements

Authors acknowledge the internal research grant from Pandit Deendayal Petroleum University (PDPU) and Solar Research & Development Centre, PDPU for providing XRD and FE-SEM facilities. Prof. Indrajit Mukhopadhyay is gratefully acknowledged for his advices on Photoelectrochemical measurements.

References

1 P. Sinsermsuksakul, K. Hartman, S. B. Kim, J. Heo, L. Sun, H. H. Park, R. Chakraborty, T. Buonassisi and R. G. Gordon, *Appl. Phys. Lett.*, 2013, **102**, 053901.
2 Y. Sun, Z. Sun, S. Gao, H. Cheng, Q. Liu, F. Lei, S. Wei and Y. Xie, *Adv. Energy Mater.*, 2014, **4**, 1–11.
3 M. Patel, I. Mukhopadhyay and A. Ray, *Opt. Mater.*, 2013, **35**, 1693–1699.
4 M. Sugiyama, K. Reddy, N. Revathi, Y. Shimamoto and Y. Murata, *Thin Solid Films*, 2011, **519**, 7429–7431.
5 W. Wang, K. Leung, W. Fong, S. Wang, Y. Hui, S. Lau, Z. Chen, L. Shi, C. Cao and C. Surya, *J. Appl. Phys.*, 2012, **111**, 093520.
6 S. M. Sze and K. K. Ng, *Physics of semiconductor devices*, John Wiley & Sons, 2006.
7 J. Vidal, S. Lany, M. dAvezac, A. Zunger, A. Zakutayev, J. Francis and J. Tate, *Appl. Phys. Lett.*, 2012, **100**, 032104.
8 S. Zhang and S. Cheng, *Micro Nano let. IET*, 2011, **6**, 559–562.
9 W. Albers, C. Haas, H. Vink and J. Wasscher, *J. Appl. Phys.*, 1961, **32**, 2220–2225.
10 M. Devika, N. K. Reddy, K. Ramesh, K. Gunasekhar, E. Gopal and K. R. Reddy, *J. Electrochem. Soc*, 2006, **153**, G727–G733.
11 H. J. Jia, S. Y. Cheng and P. M. Lu, *Adv. Mat. Res.*, 2011, **152**, 752–755.
12 M. Reghima, A. Akkari, C. Guasch and N. Kamoun-Turki, *J. Renewable Sustainable Energy*, 2012, **4**, 011602.
13 W. Huang, S. Cheng and H. Zhou, *ECS Trans.*, 2012, **44**, 1295–1301.
14 S. Zhang, S. Y. Cheng, H. J. Jia and H. F. Zhou, *Adv. Mat. Res.*, 2012, **418**, 712–716.
15 V. Gremenok, V. Y. Rud, Y. V. Rud, S. Bashkirov and V. Ivanov, *Semiconductors*, 2011, **45**, 1053–1058.
16 A. Dussan, F. Mesa and G. Gordillo, *J. Mater. Sci.*, 2010, **45**, 2403–2407.
17 P. Sinsermsuksakul, R. Chakraborty, S. B. Kim, S. M. Heald, T. Buonassisi and R. G. Gordon, *Chem. Mater.*, 2012, **24**, 4556–4562.
18 K. Santhosh Kumar, C. Manoharan, S. Dhanapandian and A. Gowri Manohari, *Spectrochim. Acta, Part A*, 2013, **115**, 840–844.
19 M. F. Weber and M. J. Dignam, *J. Electrochem. Soc.*, 1984, **131**, 1258–1265.
20 K. Sivula and M. Gratzel, *Photoelectrochemical Water Splitting: Materials, Processes and Architectures*, 2013, 83.
21 P. Sinsermsuksakul, J. Heo, W. Noh, A. S. Hock and R. G. Gordon, *Adv. Energy Mater.*, 2011, **1**, 1116–1125.
22 A. Schneikart, H. Schimper, A. Klein and W. Jaegermann, *J. Phys. D: Appl. Phys.*, 2013, **46**, 305109.
23 K. Ramakrishna Reddy, N. Koteswara Reddy and R. Miles, *Sol. Energy Mater. Sol. Cells*, 2006, **90**, 3041–3046.
24 M. Patel, I. Mukhopadhyay and A. Ray, *J. Phys. D: Appl. Phys.*, 2012, **45**, 445103.
25 A. Bradley and A. Jay, *Proc. Phys. Soc.*, 1932, **44**, 563.
26 S. Prabahar and M. Dhanam, *J. Cryst. Growth*, 2005, **285**, 41–48.
27 D. Dye, H. Stone and R. Reed, *Curr. Opin. Solid State Mater. Sci.*, 2001, **5**, 31–37.
28 P. Tyagi and A. Vedeshwar, *Phys. Rev. B: Condens. Matter*, 2002, **66**, 075422.
29 S. Zimin, E. Gorlachev, I. Amirov, V. Naumov, G. Dubov, V. Gremenok and S. Bashkirov, *Semicond. Sci. Technol.*, 2014, **29**, 015009.
30 J. Sharma, G. SAINT, N. Goyal and S. Tripathi, *J. Optoelectron. and Adv. M.*, 2007, **9**, 3194–3199.
31 M. Patel, I. Mukhopadhyay and A. Ray, *Semicond. Sci. Technol.*, 2013, **28**, 055001.
32 M. Patel and A. Ray, *ACS Appl. Mater. Interfaces*, 2014, **6**, 10099–10106.

TOC entry document:

Title:

"Magnetron sputtered Cu doped SnS thin films for improved photoelectrochemical and heterojunction solar cells"

Malkeshkumar Patel and Abhijit Ray

Graphical Abstract

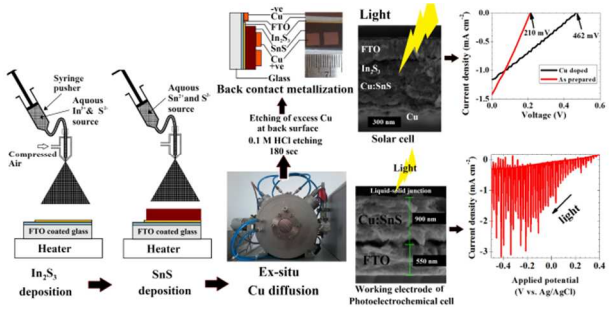

Novelty statement:

Ex-situ Cu-doped SnS demonstrating large J_{ph} = 3.2mA/cm^2 as photocathode and enhanced V_{OC} = 465 mV in hetero-junction solar cell.